The EMBO Journal (2006) 25, 900–909 | © 2006 European Molecular Biology Organization | All Rights Reserved 0261-4189/06
www.embojournal.org

THE EMBO JOURNAL

AtSufE is an essential activator of plastidic and mitochondrial desulfurases in *Arabidopsis*

Xiang Ming Xu[1] and Simon Geir Møller[1,2,*]

[1]Department of Mathematics and Natural Science, University of Stavanger, Stavanger, Norway and [2]Department of Biology, University of Leicester, Leicester, UK

Iron–sulfur (Fe–S) clusters are vital prosthetic groups for Fe–S proteins involved in fundamental processes such as electron transfer, metabolism, sensing and signaling. In plants, sulfur (SUF) protein-mediated Fe–S cluster biogenesis involves iron acquisition and sulfur mobilization, processes suggested to be plastidic. Here we have shown that AtSufE in *Arabidopsis* rescues growth defects in SufE-deficient *Escherichia coli*. In contrast to other SUF proteins, AtSufE localizes to plastids and mitochondria interacting with the plastidic AtSufS and mitochondrial AtNifS1 cysteine desulfurases. AtSufE activates AtSufS and AtNifS1 cysteine desulfurization, and AtSufE activity restoration in either plastids or mitochondria is not sufficient to rescue embryo lethality in *AtSufE* loss-of-function mutants. AtSufE overexpression induces *AtSufS* and *AtNifS1* expression, which in turn leads to elevated cysteine desulfurization activity, chlorosis and retarded development. Our data demonstrate that plastidic and mitochondrial Fe–S cluster biogenesis shares a common, essential component, and that AtSufE acts as an activator of plastidic and mitochondrial desulfurases in *Arabidopsis*.
The EMBO Journal (2006) **25,** 900–909. doi:10.1038/sj.emboj.7600968; Published online 26 January 2006
Subject Categories: plant biology
Keywords: *Arabidopsis*; desulfurization; iron–sulfur cluster formation; mitochondria; plastids

Introduction

Iron–sulfur (Fe–S) clusters represent important and versatile prosthetic groups of Fe–S proteins involved in processes such as electron transport, redox and non-redox catalysis, sensing, signalling, DNA repair and regulation of gene expression (Beinert and Kiley, 1999; Balk and Lobreaux, 2005; Lill and Muhlenhoff, 2005). Although simple in structure, Fe–S biosynthesis requires the interplay of numerous proteins (Lill and Kispal, 2000; Frazzon and Dean, 2003; Balk and Lobreaux, 2005).

Fe–S cluster biogenesis is divided into elemental sulfur formation, iron acquisition, assembly of sulfur and iron into a cluster, and cluster insertion into apoproteins (Johnson *et al*, 2005; Lill and Muhlenhoff, 2005). Most research has come from bacteria which contain three main systems termed nitrogen fixation (NIF), iron–sulfur cluster (ISC) and mobilization of sulfur (SUF) (Balk and Lobreaux, 2005). Initial research came from studies in *Azetobacter vinelandii* (Frazzon and Dean, 2003), where the nitrogenase requires Fe–S cluster assembly by the cysteine desulfurase NifS. The NIF system is specifically involved only in the assembly and maturation of nitrogenase Fe–S clusters (Jacobson *et al*, 1989). The ISC system is more general and *isc* operon (*iscSUA-hscBA-fdx*) mutations in *Escherichia coli* result in decreased activities of numerous Fe–S proteins (Zheng *et al*, 1998; Schwartz *et al*, 2000; Tokumoto and Takahashi, 2001). In contrast to the NIF system, ISC components have been found in bacteria and higher eukaryotes (Muhlenhoff and Lill, 2000; Balk and Lobreaux, 2005).

The *suf* operon (*sufABCDSE*) represents the third Fe–S system, which can partially complement the *isc* operon (Takahashi and Tokumoto, 2002). SufB, SufC and SufD are conserved proteins, and in bacteria the cytosolic SufC ATPase interacts with SufB and SufD, presumably acting as an energizer for iron acquisition during Fe–S assembly (Loiseau *et al*, 2003; Nachin *et al*, 2003). Further, SufE interacts with SufS, where SufE accepts sulfur mobilized from cysteine and SufE/SufS may form a two-component cysteine desulfurase (Loiseau *et al*, 2003; Outten *et al*, 2003). Once acquired, SufA can assemble Fe–S clusters transiently *in vitro* (Ollagnier-de-Choudens *et al*, 2003).

In yeast and mammals all Fe–S clusters are thought to be generated in mitochondria, although this is still debated (Lill and Kispal, 2000; Rouault and Tong, 2005). In plants there is evidence that mitochondria harbor an Fe–S cluster biogenesis system involving the ABC transporter Sta1 and the putative cysteine desulfurase AtNifS1 (AtNSF1) (Kushnir *et al*, 2001). Indeed, the potato mitochondrial NifS homolog can activate biotin synthase (Picciocchi *et al*, 2003). The existence of the *Arabidopsis* chloroplast-localized Nif-like protein AtCpNIFS/AtNFS2/AtSufS and mitochondrial and plastidic NFU Fe–S cluster biogenesis proteins demonstrates that Fe–S cluster assembly in plants involves both mitochondria and plastids (Leon *et al*, 2002, 2003; Pilon-Smits *et al*, 2002).

Recently, homologs of the bacterial *suf* operon were identified in *Arabidopsis*, all of which appear to be plastid localized. AtSufC/AtNAP7 is a plastidic ABC/ATPase essential for *Arabidopsis* embryogenesis, which can rescue SufC deficiency in *E. coli* (Xu and Møller, 2004). AtSufC/AtNAP7 interacts with AtSufD/AtNAP6 and AtSufB/AtNAP1 in plastids (Xu *et al*, 2005), and this SufBCD complex may act as an energizer during iron acquisition. AtSufD/AtNAP6 also plays an essential role during *Arabidopsis* embryogenesis (Hjorth *et al*, 2005). Furthermore, the SufA-like protein CpIscA may act as a plastidic scaffold protein during Fe–S cluster assembly (Abdel-Ghany *et al*, 2005). Although the *Arabidopsis* genome harbors a SufE homolog, no data exist on this protein.

*Corresponding author. Department of Mathematics and Natural Science, University of Stavanger, 4036 Stavanger, Norway.
E-mail: simon.g.moller@uis.no

Received: 25 August 2005; accepted: 22 December 2005; published online: 26 January 2006

In chloroplasts Fe–S clusters are paramount for the functioning of cytochrome b/f complex, ferredoxin and photosystem I, ensuring thylakoid electron transport (Kapazoglou *et al*, 2000). The chloroplast import protein Tic55 also contains an Fe–S cluster (Caliebe *et al*, 1997). The requirement for Fe–S proteins to be part of multiple cellular processes argues that Fe–S cluster biogenesis is an essential part of plant development. Although recent studies have shed light on SUF-mediated iron acquisition in plastids, little is known regarding sulfur mobilization. Similarly, the intercompartmental coordination of plastidic and mitochondrial Fe–S cluster systems remains unexplored. Here we show that AtSufE in *Arabidopsis* represents an evolutionarily conserved SufE protein that, in contrast to other SUF proteins, localizes to both plastids and mitochondria, where it interacts with and activates the plastidic AtSufS and mitochondrial AtNifS1 desulfurases. AtSufE-mediated desulfurization activation is essential in both organelles, and we propose that AtSufE may act as an interorganellar coordinator of Fe–S cluster biogenesis in plants.

Results

AtSufE is an evolutionarily conserved SufE protein

A full-length *Arabidopsis thaliana* cDNA (1116 nt) encoding a putative SufE-like protein was cloned, which we named AtSufE. AtSufE is a single-copy nuclear gene (At4g26500) on chromosome IV encoding a 371-amino-acid protein (NM_118783) with 49% similarity to SufE from *Nostoc punctiforme* (NP_487553) and 27% similarity to *E. coli* SufE (NP_416194) (Figure 1B). In constrast to *E. coli* and *N. punctiforme* SufE, AtSufE contains a 150-amino-acid C-terminal extension, 88 amino acids of which show 41% similarity to the *E. coli* BolA protein (NP_487553) (Figure 1B). In *E. coli*, BolA acts as a morphogen, with overexpression resulting in spherical cells during starvation (Aldea *et al*, 1988); however, overexpression of the AtSufE BolA domain in isolation has no effect in *E. coli* or *Arabidopsis* (data not shown), indicating that the AtSufE BolA domain is a nonfunctional evolutionary relic.

To test whether AtSufE represents an evolutionarily conserved SufE protein, we analyzed whether AtSufE could complement SufE-deficient *E. coli* during iron starvation. We generated an *E. coli SufE* mutant (MG1655ΔSufE) and compared its growth characteristics to wild type (WT) (MG1655) in the presence of the iron chelator 2,2′dipyridyl. MG1655ΔSufE is unable to grow in the absence of iron, while MG1655 shows no growth differences (Figure 2A). We then analyzed the effect of AtSufE expression in MG1655ΔSufE cells (MG1655ΔSufE AtSufE) in the absence of iron, revealing that AtSufE can complement the growth defects in SufE-deficient *E. coli* (Figure 2A).

To test whether the AtSufE SufE domain is functional, we expressed the 220-amino-acid SufE domain (Figure 1B) in MG1655ΔSufE. This strain (MG1655ΔSufE AtSufE-E) was grown alongside MG1655 and MG1655ΔSufE cells in minimal A media containing 2,2′dipyridyl. MG1655ΔSufE shows growth retardation compared to MG1655, while MG1655ΔSufE AtSufE-E cells show partial complementation (Figure 2B). Combined, these data demonstrate that AtSufE is an evolutionarily conserved SufE protein.

AtSufE localizes to both plastids and mitochondria

AtSufE contains a 66-amino-acid N-terminal extension predicted to be a plastid-targeting transit peptide (P-TP) (Figure 1B). However, further predictions revealed a 30-amino-acid mitochondrial-targeting transit peptide, suggesting dual targeting (Figure 1B). To test this, constructs containing the full-length *AtSufE* cDNA fused to YFP were transiently expressed in tobacco and *Arabidopsis*, and analysis revealed fluorescence in both chloroplasts and mitochondria, demonstrating dual targeting (Figure 3A). To verify that both the plastid- and mitochondrial-targeting signals were present in the N-terminal extension, a truncated version of

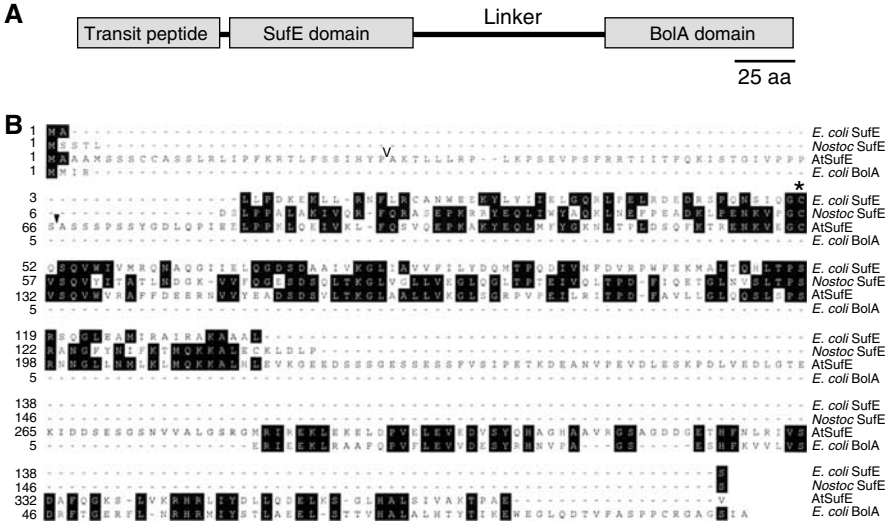

Figure 1 AtSufE is a SufE homolog. (**A**) The AtSufE domain structure showing the presence of the transit peptide, the SufE and BolA domain. (**B**) The N-terminal region of AtSufE shows similarity to SufE proteins from *E. coli* (*E. coli* SufE) and *N. punctiforme* (*Nostoc* SufE), while the 88-amino-acid C-terminal region shows similarity to *E. coli* BolA (*E. coli* BolA). The SufE and BolA domains are separated by a 62-amino-acid linker region. AtSufE contains the conserved cysteine residue (amino acid 128, asterisk) found in other SufE proteins. The open arrowhead indicates the mitochondrial transit peptide and the filled arrowhead indicates the full-length transit peptide.

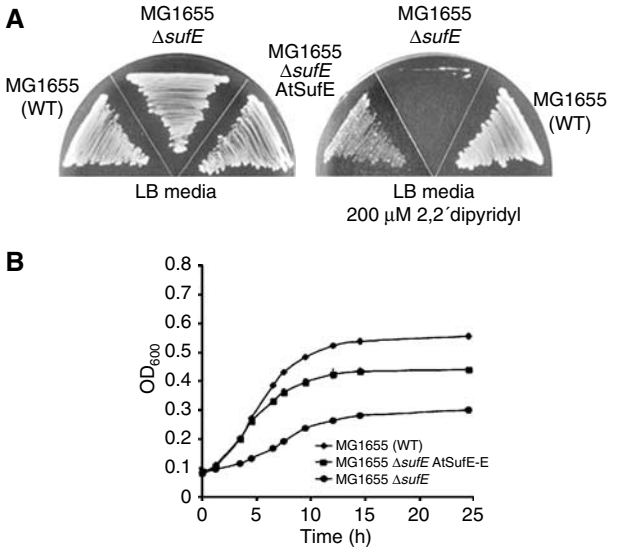

Figure 2 AtSufE is evolutionarily conserved. (**A**) Complementation of SufE-deficient *E. coli* with AtSufE during iron starvation. WT *E. coli* (MG1655), SufE-deficient *E. coli* (MG1655ΔSufE) and MG1655ΔSufE expressing AtSufE (MG1655ΔSufE AtSufE) were plated on LB media and on LB media containing 200 μM 2,2′dipyridyl. On LB media all strains grew equally well. On LB media lacking iron MG1655ΔSufE showed no growth, while expression of AtSufE in MG1655ΔSufE restored growth, demonstrating complementation. (**B**) Complementation of MG1655ΔSufE by the SufE domain. MG1655, MG1655ΔSufE and MG1655ΔSufE expressing the AtSufE SufE domain (MG1655ΔSufE AtSufE-E) were grown in minimal A media with 2,2′dipyridyl, showing that the AtSufE SufE domain has retained its activity.

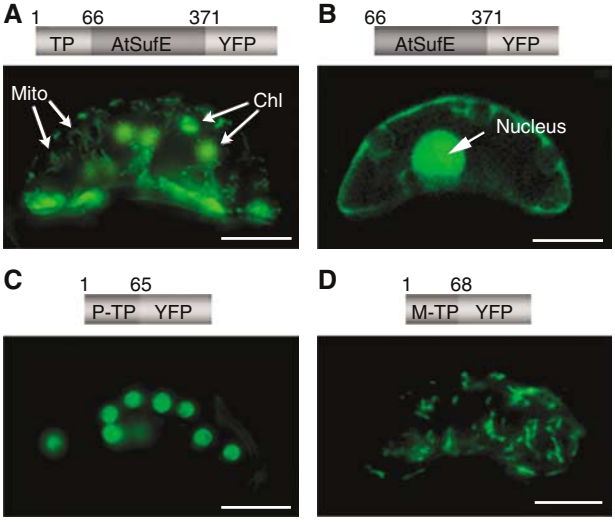

Figure 3 AtSufE localizes to both plastid and mitochondria. All constructs were transiently expressed in tobacco leaves and YFP fluorescence is shown. (**A**) Full-length AtSufE-YFP localizes to chloroplasts (Chl) and mitochondria (Mito). (**B**) Removal of the 66-amino-acid transit peptide results in cytosolic distribution. The nucleus is indicated. (**C**) Expression of the 65-amino-acid AtSufC plastid-targeting transit peptide fused to YFP, demonstrating chloroplast structures. (**D**) Expression of the 68-amino-acid mitochondrial β subunit ATP synthase signal peptide fused to YFP, demonstrating mitochondrial structures. Scale bar = 10 μm.

AtSufE lacking the 66-amino-acid N-terminus ($AtSufE_{trun}$) was fused to YFP, showing cytosolic localization (Figure 3B). To validate the observed cellular structures, the 65-amino-acid P-TP of AtSufC/AtNAP7 (Xu and Møller, 2004) and the 68-amino-acid mitochondrial-targeting transit peptide (M-TP) of the mitochondrial β subunit ATP synthase (Boutry *et al*, 1987) were fused to YFP. Transient expression analysis verified that the cellular structures showing AtSufE localization are indeed chloroplasts (Figure 3C) and mitochondria (Figure 3D). These results demonstrate that AtSufE is localized to both plastids and mitochondria.

AtSufE is essential for normal embryo development

To analyze the function of AtSufE in *Arabidopsis*, we identified two SALK (The Salk Institute, USA) T-DNA insertion lines N800113 and N511580 (Alonso *et al*, 2003), containing T-DNA insertions in *AtSufE* (Figure 4). To verify the T-DNA insertion sites, *AtSufE*- and *T-DNA*-specific primers (Figure 4A) were used to PCR amplify the flanking regions (Figure 4B). N800113 has two adjacent T-DNAs at nucleotide positions 450 and 479, while N511580 contains one T-DNA at nucleotide position 657 (Figure 4A).

We investigated seed structures in developing seed pods (siliques) in segregating populations of N800113 and N511580 plants. Siliques from heterozygous T3 populations were dissected, showing that, in contrast to uniformly developing green seeds in WT (Figure 4C), heterozygous *atsufE* siliques contained aborted seeds (Figure 4C). This phenotype was identical in N800113 and N511580 siliques (Figure 4C), showing a 3:1 ratio of viable to nonviable seeds. This is consistent with a recessive lethal segregation of embryos homozygous for the *AtSufE* T-DNA.

WT and homozygous N511580 embryos were further compared at the same developmental stages (same siliques). In general, N511580 embryos showed retarded development (Figure 4D): At the WT two–four-cell stage N511580 embryos had only reached initial zygote division, and at the WT eight-cell stage N511580 embryos had only reached the four-cell stage (Figure 4D). N511580 embryos never progressed beyond the preglobular eight-cell stage (Figure 4D). To analyze the ultrastructure of WT and N511580 preglobular embryos, we performed electron microscopy. N511580 embryo cells were more vacuolated than WT; however, the morphology and number of plastids and mitochondria were similar in WT and N511580 (Figure 4E), indicating that AtSufE loss of function does not disrupt overall organelle morphology as in AtSufC-deficient embryos (Xu and Møller, 2004).

Although N800113 and N511580 mutants showed identical phenotypes, we transformed a CaMV35S-*AtSufE* WT transgene into heterozygous N511580 plants for complementation. Seven out of 10 transgenic plants analyzed showed embryo development restoration and a 15:1 ratio of viable to nonviable seeds (Figure 4F), demonstrating that the embryo lethality is due to AtSufE deficiency.

AtSufE activity restoration in plastids or mitochondria is not sufficient to re-establish embryo development

The dual targeting of AtSufE to both plastids and mitochondria is unique to the SUF system in that all other SUF proteins in *Arabidopsis* are exclusively plastid localized (Møller *et al*, 2001; Pilon-Smits *et al*, 2002; Xu and Møller, 2004; Abdel-Ghany *et al*, 2005). To analyze whether AtSufE targeting to both organelles is important for embryo development, we tested if AtSufE activity restoration in either organelle could rescue the embryo lethality in AtSufE loss-of-function

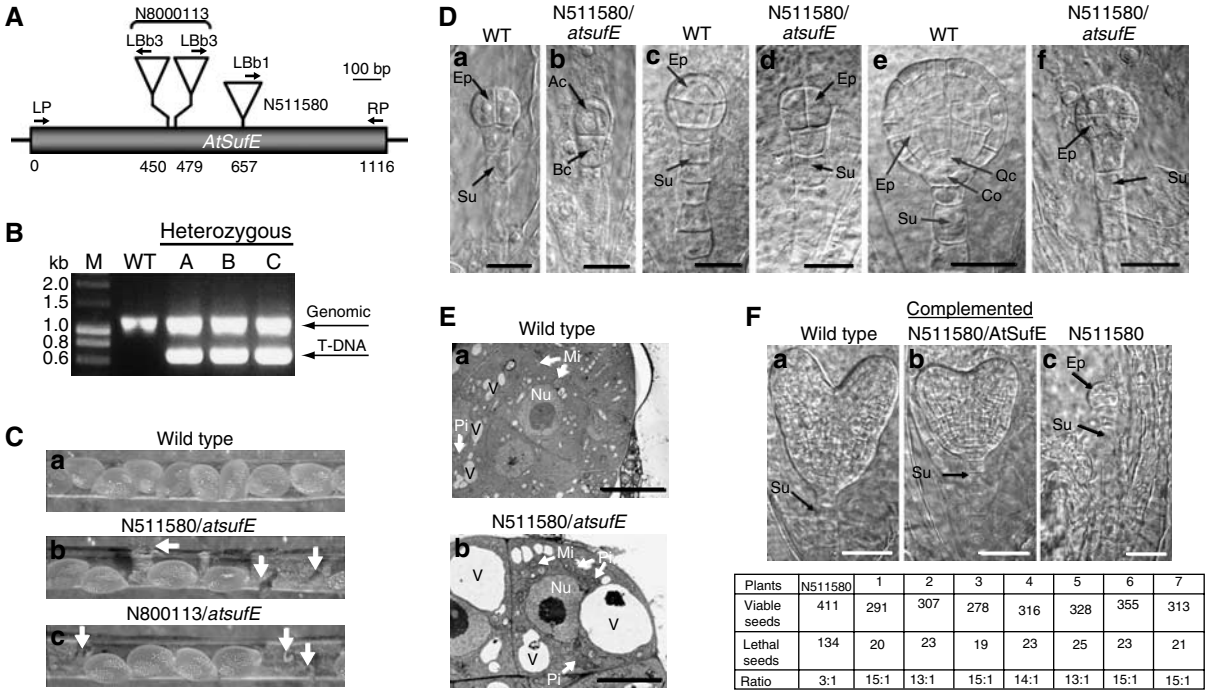

Plants	N511580	1	2	3	4	5	6	7
Viable seeds	411	291	307	278	316	328	355	313
Lethal seeds	134	20	23	19	23	25	23	21
Ratio	3:1	15:1	13:1	15:1	14:1	13:1	15:1	15:1

Figure 4 AtSufE deficiency results in abnormal seed development and arrested embryo development. (**A**) Schematic diagram showing the T-DNA insertion sites in N800113 and N511580 and primers used for molecular analysis. (**B**) PCR analysis of heterozygous N511580 using primers LBb1, RP1580 and LP1580, showing the presence of the T-DNA in N511580, its absence in WT and the presence of WT *AtSufE* (genomic) in both backgrounds. (**C**) WT siliques (**a**) showing uniform seed development and heterozygous N511580 (**b**), and N800113 (**c**) siliques showing ~25% aborted seed (white arrows). (**D**) DIC microscopy of WT and homozygous aborted seeds from the same heterozygous N511580 siliques at (**a, b**) the two–four-cell stage, (**c, d**) the eight-cell stage and (**e, f**) the globular stage. Ep, embryo proper; Su, suspensor; Ac, apical cell; Bc, basal cell; Qc, prospective quiescent center; Co, prospective columella. (**E**) Transmission electron microscopy of WT (**a**) and N511580 (**b**) preglobular embryo cells with normal undifferentiated plastids (Pl) and mitochondria (Mi). N511580 (**b**) contains large vacuoles (V). Nu, nucleus. (**F**) Expression of a *CaMV35S-AtSufE* transgene in heterozygous N511580 plants, demonstrating successful complementation. WT (**a**), complemented N511580 (**b**) and a mutant embryo (**c**) from a silique with heart-stage WT embryos are shown. Ep, embryo proper; Su, suspensor. Successful complementation was verified by determining the ratio of viable to aborted seeds, showing a 15:1 ratio. Scale bars = 20 μm in (D) and (F); 5 μm in (E).

mutants. We generated CaMV35S binary vectors containing $AtSufE_{trun}$, lacking the endogenous transit peptide (Figure 3B), fused to either the AtSufC/AtNAP7 (Xu and Møller, 2004) 65-amino-acid P-TP or to the 68-amino-acid mitochondrial-targeting transit peptide (M-TP) of the mitochondrial β subunit ATP synthase (Boutry *et al*, 1987) generating P-TP/AtSufE and M-TP/AtSufE. To verify correct targeting, P-TP/AtSufE and M-TP/AtSufE were fused to YFP and transiently expressed in tobacco leaves, showing exclusive plastid (Figure 5B) and mitochondrial (Figure 5C) localization, respectively. The P-TP/AtSufE and M-TP/AtSufE binary vectors lacking YFP, together with the CaMV35S full-length WT AtSufE binary vector as a control, were then transformed into heterozygous N511580 plants and analyzed for restoration of embryo development. Five transgenic lines from each transformation event were analyzed by RT–PCR, showing the presence of *AtSufE* (Figure 5A), *P-TP/AtSufE* (Figure 5B) or *M-TP/AtSufE* transcripts (Figure 5C). Seed phenotypes were then analyzed from all 15 transgenic plants, revealing that, in contrast to N511580 plants transformed with *AtSufE* showing embryo development restoration (15:1 ratio; Figure 5A), mutants transformed with either *P-TP/AtSufE* (Figure 5B) or *M-TP/AtSufE* (Figure 5C) showed a seed phenotype (ratio 3:1) similar to the *AtSufE* loss-of-function mutants. Further analysis revealed that embryos in *P-TP/AtSufE* or *M-TP/AtSufE* plants were unable to progress beyond the preglobular stage (data not shown).

As a control to ensure that both P-TP/AtSufE and M-TP/AtSufE are functional proteins in their respective organelles, we assayed whether the two separate transgenes could rescue the homozygous *N511580* mutant lethal phenotype. Heterozygous plants containing either the P-TP/AtSufE or the M-TP/AtSufE transgenes were crossed by pollination and the resulting seed screened for viability. In all, 20 viable seedlings were analyzed by RT–PCR, revealing that two seedlings (Figure 5D; seedlings A and B) did not contain the WT *AtSufE* transcript but showed the presence of *P-TP/AtSufE* and *M-TP/AtSufE* transcripts (Figure 5D). The fact that the two independent transgenes can fully complement the homozygous N511580 mutant (Figure 5D) demonstrates that both the plastid-localized and the mitochondria-localized AtSufE proteins used in this experiment are functional in their respective organelles.

AtSufE interacts with AtSufS and AtNifS1 in vivo

To test whether AtSufE could interact with the plastidic cysteine desulfurase AtSufS (Leon *et al*, 2002; Pilon-Smits *et al*, 2002; Ye *et al*, 2005) and the putative mitochondrial cysteine desulfurase AtNifS1 (Kushnir *et al*, 2001), we performed yeast two-hybrid assays. Full-length AtSufE, AtSufS and AtNifS1 proteins fused to the GAL4 activation domain (Figure 6A; AD-AtSufE, AD-AtSufS, AD-AtNifS1) and to the GAL4 DNA-binding domain (Figure 6A; BD-AtSufE, BD-AtSufS, BD-AtNifS1) were expressed in HF7c yeast cells

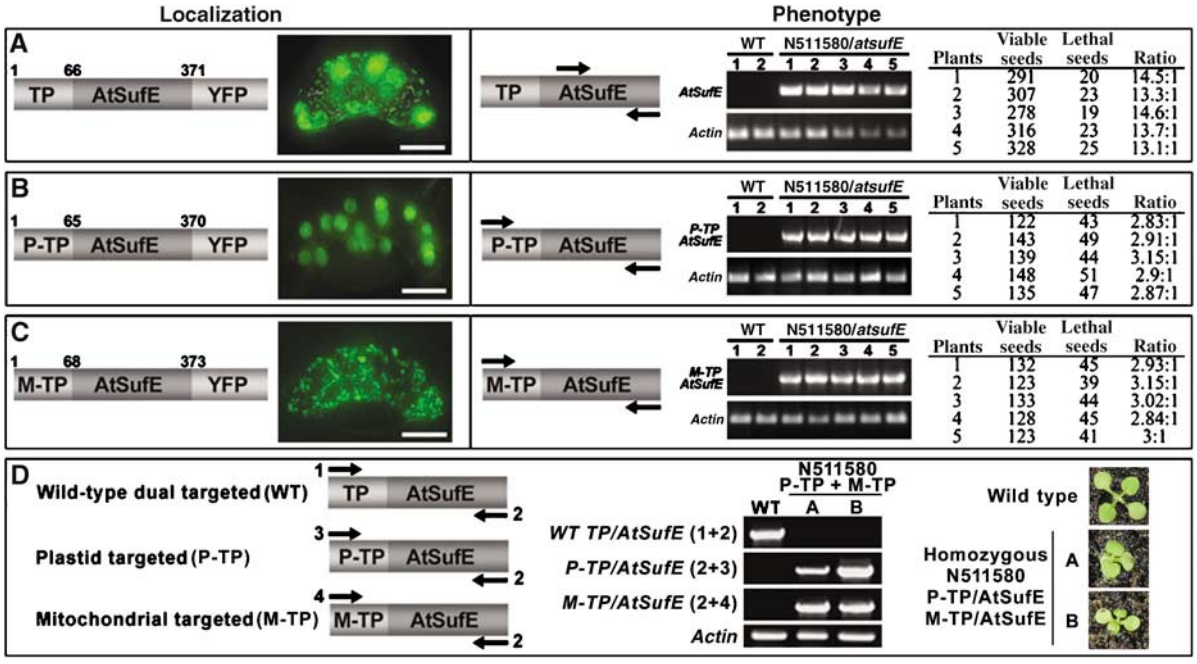

Figure 5 Normal embryo development requires AtSufE activity in both plastids and mitochondria. (**A**) WT TP-AtSufE-YFP, (**B**) P-TP/AtSufE-YFP, and (**C**) M-TP/AtSufE-YFP showing correct organelle targeting in tobacco. WT TP-AtSufE, P-TP/AtSufE and M-TP/AtSufE binary vectors were transformed into heterozygous N511580 and analyzed by RT–PCR, showing the presence of (A) WT *TP-AtSufE*, (B) *P-TP/AtSufE* and (C) *M-TP/AtSufE* transcripts. Seed phenotypes were analyzed, demonstrating that, in contrast to N511580 transformed with WT *AtSufE* (A; 15:1 ratio), N511580 transformed with either *P-TP/AtSufE* (B) or *M-TP/AtSufE* (C) showed a seed phenotype (ratio 3:1) similar to N511580. (**D**) Successful complementation of N511580 by both the *P-TP/AtSufE* and *M-TP/AtSufE* transgenes. RT–PCR analysis of homozygous N511580 plants (A, B), revealing the absence of WT *TP-AtSufE* but the presence of both *P-TP/AtSufE* and *M-TP/AtSufE* transcripts. WT and complemented viable seedlings are shown.

and monitored for growth in the absence of histidine (His) as a marker for protein–protein interaction. His auxotrophy was restored in cells coexpressing AD-AtSufE/BD-AtSufS and AD-SufS/BD-AtSufE, demonstrating that AtSufE interacts with AtSufS (Figure 6A). Furthermore, cells coexpressing AD-AtSufE/BD-AtNifS1 and AD-AtNifS1/BD-AtSufE showed growth on media lacking His (−HTL), revealing that AtSufE also interact with AtNifS1 (Figure 6A). Yeast cells coexpressing the AD or BD vectors with BD-AtSufE, BD-AtSufS, BD-AtNifS1 or AD-AtSufE, AD-AtSufS, AD-AtNifS1, respectively, showed no growth on -HTL media (Figure 6A). To gain insight into the relative interaction strengths, the ratio of yeast growth on media lacking tryptophan and leucine (-TL) to growth on -HTL media was determined, revealing that the AtSufE/AtSufS interaction is stronger than the AtSufE/AtNifS1 interaction.

To confirm the observed protein interactions in living plant cells, we performed bimolecular fluorescence complementation (BiFC) assays (Hu *et al*, 2002) based on the reconstitution of YFP fluorescence when nonfluorescent N-terminal (N-YFP) and C-terminal (C-YFP) YFP fragments are brought together by two interacting proteins. AtSufE fused to the N-terminus of N-YFP and AtSufS and AtNifS1 fused to the N-terminus of C-YFP were expressed in tobacco leaves. Cells coexpressing AtSufE-N-YFP and AtSufS-C-YFP showed YFP fluorescence in chloroplasts, while cells coexpressing AtSufE-N-YFP and AtNifS1-C-YFP showed YFP fluorescence in mitochondria (Figure 6B), demonstrating that AtSufE interacts with AtSufS and AtNifS1 *in planta*. To ensure that the restored fluorescence was not due to nonspecific interactions, we coexpressed AtSufE-N-YFP with the plastid-localized AtNAP7-C-YFP (Xu and Møller, 2004), two proteins that show no interaction in yeast cells, observing no fluorescence (data not shown).

AtSufS- and AtNifS1-mediated cysteine desulfurization is activated by AtSufE

The interaction of AtSufE with AtSufS and AtNifS1 prompted us to analyze whether AtSufE could stimulate cysteine desulfurization. We expressed and purified 6xHis-AtSufE, 6xHis-AtSufS and 6xHis-AtNifS1 proteins (Figure 7A) and performed *in vitro* cysteine desulfurization assays. In the absence of AtSufE, AtNifS activity was almost undetectable; however, in the presence of AtSufE cysteine desulfurization increased ∼30-fold (Figure 7B). This demonstrates not only that AtNifS1 is a cysteine desulfurase but also that activity is dependent on AtSufE activation. In constrast, AtSufS showed basal cysteine desulfurase activity in the absence of AtSufE, with an ∼7-fold increase in activity in the presence of AtSufE (Figure 7B), suggesting that AtSufE is not strictly essential for AtSufS-mediated desulfurization.

Elevated levels of AtSufE result in chlorosis and retarded plant development

To further analyze the *in vivo* role of AtSufE during Fe–S cluster biogenesis, we generated transgenic plants containing a *CaMV35S-AtSufE* transgene (Figure 8A). Four transgenic lines showing *AtSufE* overexpression (AtSufE-overexpressing (AtSufE-ox)) were analyzed, showing growth retardation and chlorosis, particularly in younger leaves and siliques (Figure 8B). As AtSufE enhances AtSufS and AtNifS1 desulfurization activity (Figure 7B), the observed phenotype

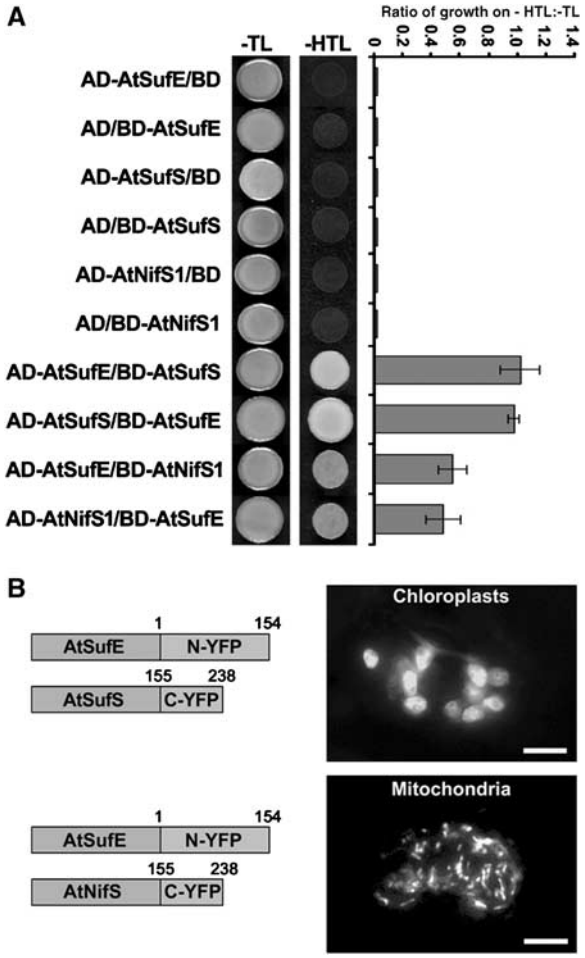

Figure 6 AtSufE interacts with plastidic AtSufS and mitochondrial AtNifS1 *in vivo*. (**A**) Yeast two-hybrid analysis of AtSufE, AtSufS and AtNifS1. Full-length AtSufE, AtSufS and AtNifS1, fused to the GAL4 activation domain (AD-AtSufE, AD-AtSufS, AD-AtNifS1) and to the GAL4 DNA-binding domain (BD-AtSufE, BD-AtSufS, BD-AtNifS1), were expressed in HF7c yeast cells and monitored for the ability to grow without histidine (-HTL media) after 3 days. Histidine auxotrophy was restored in cells coexpressing AD-AtSufE/BD-AtSufS, AD-AtSufS/BD-AtSufE, AD-AtSufE/BD-AtNifS1 and AD-AtNifS1/BD-AtSufE, showing that AtSufE interacts with AtSufS and AtNifS1 in yeast. Yeast coexpressing the above vectors with empty AD or BD vectors showed no growth on -HTL media. Relative interaction strengths were determined by measuring the ratio of growth on media lacking tryptophan and leucine (-TL) to growth on -HTL media. (**B**) BiFC assays. A nonfluorescent N-YFP fused to the C-terminus of AtSufE was transiently coexpressed in tobacco leaf cells with either AtSufS or AtNifS1 fused to the N-terminus of a nonfluorescent C-YFP. In cells expressing AtSufE-N-YFP and AtSufS-C-YFP YFP fluorescence occurs in chloroplasts, while in cells expressing AtSufE-N-YFP and AtNifS1-C-YFP fluorescence occurs in mitochondria.

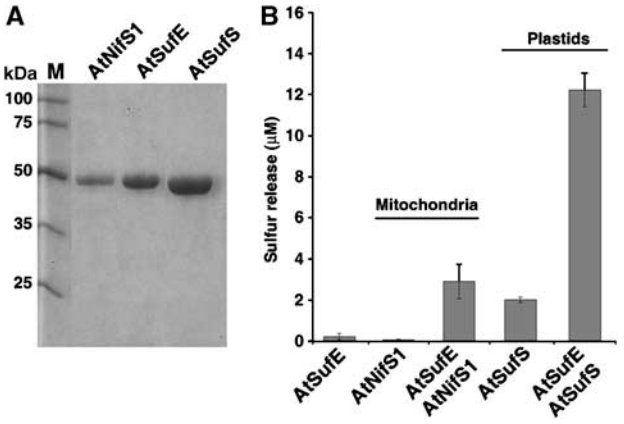

Figure 7 AtSufE acts as an activator of AtSufS- and AtNifS1-mediated cysteine desulfurization. (**A**) SDS–PAGE of purified 6xHis-AtSufE, 6xHis-AtSufS and 6xHis-AtNifS1 proteins. (**B**) Desulfurase assays using 200 nM 6xHis-AtSufS, 6xHis-AtNifS1 and 6xHis-atSufE. Methylene blue formation was measured at 670 nm. Na_2S (1–100 μM) was used for calibration and sulfur release is shown.

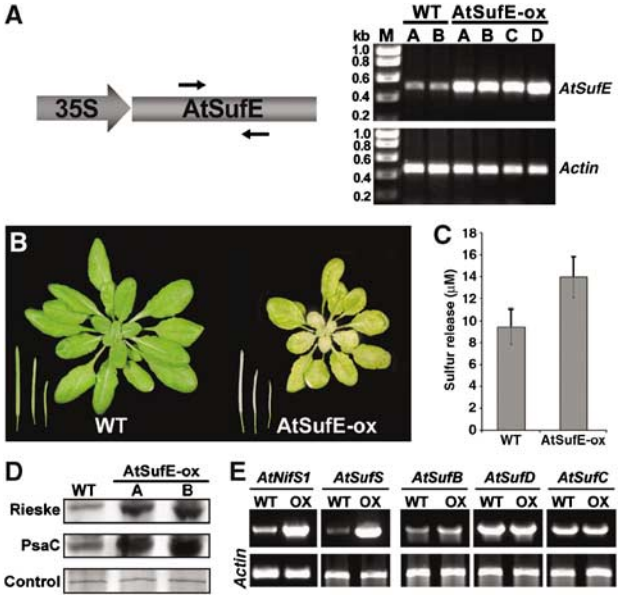

Figure 8 Overexpression of AtSufE in transgenic plants leads to retarded growth and chlorosis. (**A**) A *CaMV35S-AtSufE* binary vector was transformed into WT *Arabidopsis*. Four transgenic lines with increased *AtSufE* transcript (AtSufE-ox, A–D) compared to WT (A, B) were selected for analysis. *Actin* was used a control. (**B**) WT and AtSufE-ox plants were grown for 2 weeks on soil, revealing that AtSufE-ox plants show chlorosis and retarded growth in leaves and siliques. (**C**) *In vivo* cysteine desulfurization analysis showing that AtSufE-ox plants contain higher levels of cellular sulfur. (**D**) Western blot analysis demonstrating that the plastidic Fe–S proteins Rieske and PsaC are more abundant in AtSufE-ox plants compared to WT. (**E**) RT–PCR analysis of WT and AtSufE-ox plants showing that AtSufE overexpression results in *AtNifS1* and *AtSufS* transcript induction, while *AtSufB, AtSufD* and *AtSufC* transcript levels remain unchanged. Actin was used as control.

suggests enhanced desulfurization, resulting in increased cellular sulfide levels. To test this, we performed *in vivo* cysteine desulfurase activity assays on protein extracts from WT and AtSufE-ox plants and found significantly elevated sulfur levels in response to AtSufE overexpression (Figure 8C). To further examine whether this *in vivo* increase in cysteine desulfurization activity had an affect on Fe–S cluster-containing proteins, we carried out Western blot analysis using antibodies raised against the Rieske protein and PsaC, both plastidic Fe–S proteins. In the absence of functional Fe–S cluster biosynthesis many Fe–S proteins are unstable, and in line with this we found that elevated AtSufE-mediated cysteine desulfurase activity resulted in increased levels of both Rieske and PsaC protein (Figure 8D). This suggests that increased flux through the sulfur branch of the SUF Fe–S cluster biogenesis pathway increases

Fe–S cluster formation, ultimately leading to higher stability of Fe–S proteins.

As AtSufE stimulates AtSufS and AtNifS1 activities, we tested whether AtSufE overexpression affects *AtSufS* and *AtNifS1* levels. RT–PCR revealed that both transcripts are induced (Figure 8E), implying that increased cysteine desulfurization in AtSufE-ox plants is due to elevated levels of the AtSufE/AtSufS and AtSufE/AtNifS1 complexes. In contrast, *AtSufB*, *AtSufC* and *AtSufD* transcripts are not affected in AtSufE-ox plants (Figure 8C), suggesting that the sulfur mobilization and iron acquisition branches of the SUF protein-mediated Fe–S cluster biogenesis pathways may show independent regulation.

Discussion

SUF protein-mediated Fe–S cluster biogenesis in plastids can be divided into two main processes: iron acquisition and sulfur mobilization from cysteine. Recent studies have shed light on iron acquisition (Xu and Møller, 2004; Hjorth *et al*, 2005; Xu *et al*, 2005), but little is known about how the SUF system regulates sulfur mobilization. We have characterized AtSufE, revealing dual localization to plastids and mitochondria. AtSufE interacts with and activates the cysteine desulfurases, AtSufS in plastids and AtNifS1 in mitochondria, and both activations are vital during embryogenesis. Our data demonstrate that plastidic and mitochondrial Fe–S cluster assemblies share a common, vital component, and we propose that AtSufE acts as an interorganellar coordinator of Fe–S cluster biogenesis in *Arabidopsis*.

AtSufE is an evolutionarily conserved SufE protein in Arabidopsis with dual localization

As *E. coli* SufE mobilizes sulfur preferably under iron-limiting conditions (Outten *et al*, 2004), the finding that AtSufE can complement SufE-deficient *E. coli* in the absence of iron indicates the evolutionary conservation of the process (Figure 2A). Moreover, that the SufE domain is sufficient for complementation suggests that this domain has retained its prokaryotic SufE activity (Figure 2B). *E. coli* SufE acts as a sulfur acceptor, mobilized by SufS, where cysteine 51 is the acceptor site (Figure 1B; Outten *et al*, 2003) and AtSufE contains this conserved cysteine (Figure 1B). As AtSufE can substitute its bacterial counterpart, AtSufE-mediated sulfur mobilization probably shows similarities to that in bacteria.

Despite previous studies suggesting that the entire SUF pathway is exclusively plastid localized (Balk and Lobreaux, 2005), AtSufE is unique in that it is targeted to both plastids and mitochondria (Figure 3A). Although it is not known whether amino acids responsible for plastid and mitochondrial targeting are overlapping or separate (Chew *et al*, 2003), deletion experiments show that signals for the dual localization lie within the 66-amino-acid N-terminal extension of AtSufE (Figure 3B). Dual SUF protein localization suggests that Fe–S cluster biogenesis may be controlled by a common protein acting in both organelles.

Fe–S cluster biogenesis is an essential process in both plastids and mitochondria during embryogenesis

The embryo lethal phenotype of homozygous AtSufE loss-of-function mutants demonstrates that AtSufE is an essential protein (Figure 4D). Through yeast two-hybrid and BiFC analysis, we have shown that AtSufE interacts with AtSufS in plastids (Figure 6) and AtNifS1 in mitochondria (Figure 6), suggesting that AtSufE acts as the essential protein in the AtSufE/AtSufS and AtSufE/AtNifS1 complexes. AtSufS or AtNifS1 loss-of-function analysis has not been reported in plants; however, in *Synechocystis* sp. PCC6803 deletion of the *slr0077/SufS* gene results in only merodiploid strains (Seidler *et al*, 2001), while in *Bacillus subtilis* the SufS homolog *csd/yurw* is essential for viability (Kobayashi *et al*, 2003). This suggests that AtSufE, AtSufS and AtNifS1 may all be essential during sulfur mobilization.

The lethality in AtSufE loss-of-function embryos is more severe than that observed in AtSufC/AtNAP7 mutants. Embryo development in *atsufE* is severely retarded and arrests at the preglobular stage (Figure 4D), while *atsufC* embryos arrest at the late globular stage (Xu and Møller, 2004). The severity of the *atsufE* phenotype may simply be due to the combined loss of sulfur mobilization in both plastids and mitochondria. We suggest that AtSufE-mediated sulfur mobilization may represent a more universal step involved in different Fe–S cluster assembly pathways. To test this notion, we restored AtSufE activity specifically in plastids or mitochondria (Figure 5). Interestingly, plants harboring only plastid-targeted or only mitochondrial-targeted AtSufE (Figure 5B and C) showed no embryo development restoration (Figure 5), demonstrating that organelle-specific AtSufE re-establishment is not sufficient to allow embryo progression, revealing that AtSufE-mediated sulfur mobilization is crucial in both organelles.

Plastidic Fe–S cluster biogenesis is mediated by the SUF proteins and in mitochondria the presence of AtNifS1 and all key ISC components (cf. Balk and Lobreaux, 2005) suggests the presence of at least two pathways in both organelles. That AtSufE deficiency in either organelle results in embryo lethality (Figure 5) implies little functional redundancy between the SUF and ISC systems. This supports the notion that plants have multiple Fe–S cluster biogenesis pathways, separated in two organelles, which to date have been largely viewed as independent processes.

Activation of AtSufS and AtNifS1 cysteine desulfurization by AtSufE may coordinate Fe–S cluster biogenesis

The finding that AtSufE interacts with and activates AtSufS and AtNifS1 demonstrates that the AtSufE/AtSufS and AtSufE/AtNifS1 complexes are functional (Figure 7B). Furthermore, an increase in AtSufE results in *AtSufS* and *AtNifS1* induction (Figure 8E), suggesting a universal regulation of proteins involved in sulfur mobilization. Furthermore, it appears that correct AtSufE levels are vital in that AtSufE overexpression leads to growth retardation and chlorosis due to increased sulfur levels (Figure 8B and C).

AtNifS1 and AtSufS differ in their cysteine desulfurization activities. In the absence of AtSufE AtNifS1-mediated desulfurization is almost undetectable, while AtSufS shows significant activity in the absence of AtSufE (Figure 7B). This suggests that mitochondrial AtNifS1-mediated desulfurization is dependent on AtSufE, while plastidic AtSufS activity is not dependent, but stimulated by AtSufE. The stimulation by AtSufE in plastids is, however, essential because restoration of AtSufE in mitochondria does not result in embryo development restoration (Figure 5C). This implies that the

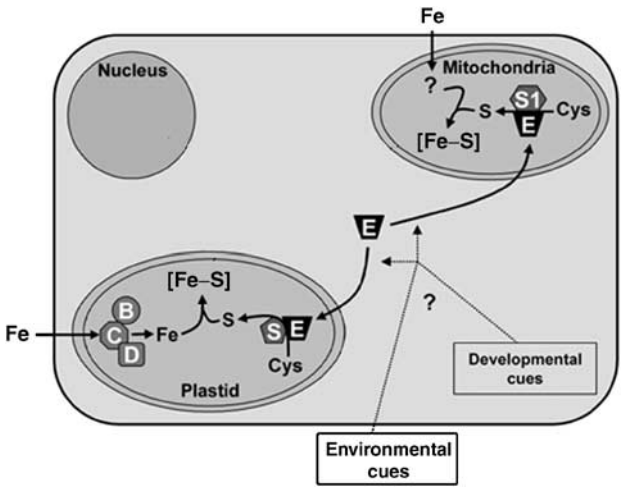

Figure 9 A working model of AtSufE-mediated coordination of Fe–S cluster biogenesis in plastids and mitochondria in *Arabidopsis.* AtSufE (E) is targeted to both plastids and mitochondria, where it interacts with plastidic AtSufS (S) and mitochondrial AtNifS1 (S1). This interaction results in activation of cysteine desulfurization by AtSufS and AtNifS1, resulting in sulfur transfer to the acquired iron to generate Fe–S clusters. The targeting of AtSufE (E) to both plastids and mitochondria may represent a control point possibly influenced by endogenous developmental cues or exogenous environmental cues.

low basal level of sulfur mobilization by AtSufS, in the absence of AtSufE, is not sufficient to support adequate Fe–S cluster biogenesis, ensuring plastid functionality.

In *E. coli*, transfer of sulfur to SufE occurs in the presence of SufS but not NifS (Outten *et al*, 2003); so why have plants evolved a common activator of sulfur mobilization in two different organelles? Plant Fe–S cluster biogenesis clearly takes place in both plastids and mitochondria (Balk and Lobreaux, 2005), and we have shown that not only is the presence of sulfur mobilization in both organelles vital but also that appropriate rates of cysteine desulfurization appear important (Figures 5 and 8). Therefore, plant cells probably require communication between plastids and mitochondria to ensure coordination and appropriate Fe–S cluster assembly rates. We propose that AtSufE may fulfil this role, acting as an interorganellar coordinator ensuring a balance between plastidic and mitochondrial Fe–S cluster biogenesis (Figure 9). As plastidic and mitochondrial Fe–S protein biogenesis varies during development, it is possible that the regulation of AtSufE-mediated cysteine desulfurization is influenced by developmental and environmental cues (Figure 9). By exploring *in vivo* Fe–S cluster synthesis rates in plastids and mitochondria, with respect to AtSufE activity, under different growth conditions and at different developmental stages, the complexity of Fe–S cluster biogenesis coordination in plants will become unraveled.

Materials and methods

Isolation of AtSufE T-DNA insertion mutants and complementation

Plants were grown on MS medium or soil under 16 h light/8 h dark cycles at 22°C. N511580 and N800113 were identified from the SALK T-DNA collection (Alonso *et al*, 2003) and genotyped by PCR using primers LP1580/LB1 (N511580) and LP1580/LB3 or RP1580/LB3 (N800113). (Primers are listed in Supplementary Table.) For complementation analysis, full-length *AtSufE* was PCR amplified with primers ATSUFE-BA-L/ATSUFE-BA-R, digested with *Xho*I and *Spe*I, cloned into the CaMV35S promoter binary vector pBA002 (Kost *et al*, 1998), and transformed into heterozygous N511580 plants using the floral-dip method (Clough and Bent, 1998).

For organelle-specific complementation, truncated *AtSufE*, lacking its transit peptide, was PCR amplified with primers ATSUFE-Trun-L/ATSUFE-BA-R, digested with *Xho*I and *Spe*I, and ligated in pBA002, resulting in pBA-trun-AtSufE. The AtSufC/AtNAP7 transit peptide was PCR amplified using primers Chl-lead-L/Chl-lead-R and the ATP synthase mitochondrial signal peptide using Mito-lead-L/Mito-lead-R, digested with *Xho*I and ligated into pBA-trun-AtSufE. For localization studies, the *AtSufE* versions were PCR amplified from pBA-Chl-trun-atSufE and pBA-Mito-trun-atSufE using primer pairs Chl-lead-L/ATSUFE-W18-R and Mito-lead-L/ATSUFE-W18-R, cloned upstream of YFP in pWEN18 and transiently expressed in tobacco.

To ensure that pBA-Chl-trun-atSufE and pBA-Mito-trun-atSufE in combination could rescue the N511580 phenotype, heterozygous N511580 plants containing pBA-Chl-trun-atSufE or pBA-Mito-trun-atSufE were genotyped for the T-DNA insertion and for either the Chl-trun-atSufE or Mito-trun-atSufE transgenes as before. Positive plants were then crossed and the seed germinated on MS media containing Basta (10 mg/l). PCR was performed using primers LBb1 with LP5180 and RP5180 to screen for homozygous seedlings. RNA was then extracted from the homozygous seedlings, followed by RT–PCR analysis using primers specific for WT *AtSufE*, *Chl-trun-atSufE* and *Mito-trun-atSufE* as described above.

Overexpression and purification of AtSufE, AtSufS and AtNifS1

Full-length *AtSufE*, *AtSufS* and *AtNifS1* cDNAs were PCR amplified using primers AtSufE-ET-L/AtSufE-ET-L, AtSufS-ET-L/AtSufS-ET-R and AtNifS-ET-L/AtNifS-ET-R, *AtSufE* digested with *Eco*RI and *Xho*I, *AtSufS* and *AtNifS* with *Bam*HI and *Xho*I, and ligated into pET28a (Novagen). The plasmids were transformed into *E. coli* Rosetta (DE3)pLysS (Novagen) and expression performed for 20 h in auto-induction ZYM-5052 media (Studier, 2005). Cells were disrupted in 50 mM Tris–HCl (pH 8.0), 25% sucrose, 5 mM $MgCl_2$, 100 mM NaCl, 1% Triton X-100 and 10 μM/ml Benzonase® Nuclease (Novagen), proteins purified using TALON affinity resin (BD Biosciences) and protein purity verified by SDS–PAGE.

Cysteine desulfurase assay

The procedure followed previous protocols (Outten *et al*, 2003) with modifications. Reactions were carried out in 50 mM Tris–HCl, pH 7.5, 5 mM $MgCl_2$ and 100 mM NaCl using 200 nM purified 6xHis-AtSufS, 6xHis-AtNifS1 and 6xHis-AtSufE. BSA (200 nM) was used as a control. Pyridoxal 5′-phosphate (10 μM) and DTT (100 μM) were used for all reactions. Reactions were initiated by adding 100 μM L-cysteine, allowed to proceed for 30 min at 30°C, and were quenched by adding 100 μl of 20 mM *N,N*-dimethyl-*p*-phenylenediamine/7.2 M HCl. The addition of 100 μl of 30 mM $FeCl_3$/1.2 M HCl followed by incubation for 20 min led to formation of methylene blue, which was measured at 670 nm. Na_2S (1–100 μM) was used for calibration.

For *in vivo* assays, WT and AtSufE-ox seedlings were grown for 2 weeks and proteins extracted as described (Pilon-smits *et al*, 2002): 2 g fresh tissue was added to 2 ml extraction buffer (50 mM Tris–HCl, pH 7.5, 100 mM NaCl, 1 mM phenylmethyl sulfonyl fluoride, 1 mM DTT, 0.5% (v/v) Triton X-100) and 100 μl of each protein solution was used for enzyme assays as described.

Western blotting

WT and two independent AtSufE-ox seedlings were grown for 2 weeks, total protein extracted, followed by Western blot analysis using antibodies raised in rabbit against the Rieske and PsaC proteins.

AtSufE localization analysis

Full-length *AtSufE* was PCR amplified using primers ATSUFE-W18-L/ATSUE-W18-R, digested with *Xho*I and *Kpn*I, cloned into pWEN18 as an N-YFP and transiently expressed in tobacco, followed by YFP fluorescence analysis on a Nikon TE-2000U inverted microscope (Nikon, Japan). As a control for targeting, the mitochondrial and plastid signal peptides were PCR amplified as before and fused to YFP in pWEN18, followed by transient expression in tobacco.

For embryo analysis, seeds were cleared for 24 h in chloral hydrate/H_2O/glycerol, 8:2:1 (w/v/v), and examined using DIC microscopy.

Electron microscopy was performed using standard protocols on a JEOL 1220 transmission electron microscope.

Generation of an E. coli SufE mutant and complementation by AtSufE

The *SufE* gene in *E. coli* strain MG1655 was disrupted using standard protocols (Datsenko and Wanner, 2000). *AtSufE* was PCR amplified using primers ATSUFE-UC-L/ATSUFE-UC-R, digested with *Pst*I and *Kpn*I and ligated in pUC19 to generate pUC-AtSufE. pUC-AtSufE-E, containing only the SufE domain of AtSufE, was generated by PCR amplification using primers ATSUFE-E-L/ATSUFE-E-R, digested with *Pst*I and *Kpn*I, and ligated in pUC19. pUC-AtSufE and pUC-AtSufE-E were transformed into MG1655Δ*sufE* to generate MG1655Δ*sufE AtSufE* and MG1655Δ*sufE AtSufE-E*. WT MG1655, MG1655Δ*sufE*, and MG1655Δ*sufE AtSufE* and MG1655Δ*sufE AtSufE-E* were grown overnight in LB medium at 37°C and plated on LB medium or used to inoculate minimal A medium containing 0.2% gluconate, 1 μg/ml thiamine and 200 μM 2,2′dipyridyl. Growth was measured at OD_{600}.

Yeast two-hybrid analysis

Full-length *AtSufE*, *AtSufS* and *AtNifS1* cDNAs were PCR amplified using primers ATSUFE-YTH-L/ATSUFE-YTH-R, ATSUFS-YTH-L/ATSUFS-YTH-R and ATNIFS1-YTH-L/ATNIFS1-YTH-R, *AtSufE* and *AtNifS1* digested with *Eco*RI and *Bam*HI, *AtSufS* with *Nde*I and *Bam*HI, and cloned into pGADT7 and pGBKT7. Plasmids and empty vector controls were transformed into HF7c yeast cells and tested for restoration of His auxotrophy (Matchmaker two-hybrid system, version 3, Clontech).

Bimolecular fluorescence complementation

Full-length *AtSufE* was PCR amplified using primers ATSUFE-W18-L/ATSUFE-W18-R, digested with *Xho*I and *Kpn*I, and cloned into pWEN-N-YFP (containing amino acids 1–154 of YFP), generating pWEN-AtSufE-N-YFP. Full-length *AtSufS* and *AtNifS1* were PCR amplified using primers ATSUFS-WEN-L/ATSUFS-WEN-R and ATNIFS1-NY-L/ATNIFS1-NY-R, digested with *Xho*I and *Kpn*I, and cloned into pWEN-C-YFP separately. pWEN-AtSufE-N-YFP/pWEN-AtSufS-C-YFP and pWEN-AtSufE-N-YFP/pWEN-AtNifS1-C-YFP were transiently expressed in tobacco in separate experiments and analyzed for YFP fluorescence.

Phenotypic analysis of AtSufE-ox plants

Full-length *AtSufE* was amplified using primers ATSUFE-W18-L/ATSUFE-BA-R, digested with *Xho*I and *Spe*I, ligated in pBA002, followed by transformation into *Arabidopsis* using the floral-dip method (Clough and Bent, 1998). WT and AtSufE-ox seeds were germinated on MS medium containing Basta (10 mg/l), transferred to soil after 10 days and phenotypes recorded after 2 weeks. RT–PCR was performed to analyze expression of *AtSufB*, *AtSufD*, *AtSufC*, *AtSufS* and *AtNifS1* in WT and AtSufE-ox plants using primers ATNAP1-L/ATNAP1-R, ATNAP6-L/ATNAP6R, ATNAP7-L/ATNAP7-R, ATSUFS-L/ATSUFS-R and ATNIFS1-L/ATNIFS1-R. Actin was used as a control (primer ACT8L/ACT8R).

Supplementary data

Supplementary data are available at *The EMBO Journal* Online.

Acknowledgements

We thank the Salk Institute Genomic Analysis Laboratory for providing the sequence-indexed *Arabidopsis* T-DNA insertion mutants, NASC for providing seeds, Natalie Allcock and Stefan Hyman for electron microscopy, Sarah Deacon and Mike McPherson for auto-induction protocols, and Trudie Allen for crossing. We thank Ralf Bernd Klösgen for the Rieske protein antibody and Henrik Scheller for the PsaC antibody. This work was supported by grants from the BBSRC (91/P16510 and BB/C00552X/1) and The Royal Society (574006.G503/23280/SM) to SGM. SGM is the recipient of an EMBO Young Investigator Award.

References

Abdel-Ghany SE, Ye H, Garifullina GF, Zhang L, Pilon-Smits EA, Pilon M (2005) Iron–sulfur cluster biogenesis in chloroplasts. Involvement of the scaffold protein CpIscA. *Plant Physiol* **138:** 161–172

Aldea M, Hernandez-Chico C, de la Campa AG, Kushner SR, Vicente M (1988) Identification, cloning, and expression of bolA, an ftsZ-dependent morphogene of *Escherichia coli*. *J Bacteriol* **170:** 5169–5176

Alonso JM, Stepanova AN, Leisse TJ, Kim CJ, Chen H, Shinn P, Stevenson DK, Zimmerman J, Barajas P, Cheuk R, Gadrinab C, Heller C, Jeske A, Koesema E, Meyers CC, Parker H, Prednis L, Ansari Y, Choy N, Deen H, Geralt M, Hazari N, Hom E, Karnes M, Mulholland C, Ndubaku R, Schmidt I, Guzman P, Aguilar-Henonin L, Schmid M, Weigel D, Carter DE, Marchand T, Risseeuw E, Brogden D, Zeko A, Crosby WL, Berry CC, Ecker JR (2003) Genome-wide insertional mutagenesis of *Arabidopsis thaliana*. *Science* **301:** 653–657

Balk J, Lobreaux S (2005) Biogenesis of iron–sulfur proteins in plants. *Trends Plant Sci* **10:** 324–331

Beinert H, Kiley PJ (1999) Fe–S proteins in sensing and regulatory functions. *Curr Opin Chem Biol* **3:** 152–157

Boutry M, Nagy F, Poulsen C, Aoyagi K, Chua NH (1987) Targeting of bacterial chloramphenicol acetyltransferase to mitochondria in transgenic plants. *Nature* **328:** 340–342

Caliebe A, Grimm R, Kaiser G, Lubeck J, Soll J, Heins L (1997) The chloroplastic protein import machinery contains a Rieske-type iron–sulfur cluster and a mononuclear iron-binding protein. *EMBO J* **16:** 7342–7350

Chew O, Rudhe C, Glaser E, Whelan J (2003) Characterization of the targeting signal of dual-targeted pea glutathione reductase. *Plant Mol Biol* **53:** 341–356

Clough SJ, Bent AF (1998) Floral dip: a simplified method for *Agrobacterium*-mediated transformation of *Arabidopsis thaliana*. *Plant J* **16:** 735–743

Datsenko KA, Wanner BL (2000) One-step inactivation of chromosomal genes in *Escherichia coli* K-12 using PCR products. *Proc Natl Acad Sci USA* **97:** 6640–6645

Frazzon J, Dean DR (2003) Formation of iron–sulfur clusters in bacteria: an emerging field in bioinorganic chemistry. *Curr Opin Chem Biol* **7:** 166–173

Hjorth E, Hadfi K, Zauner S, Maier UG (2005) Unique genetic compartmentalization of the SUF system in cryptophytes and characterization of a SufD mutant in *Arabidopsis thaliana*. *FEBS Lett* **579:** 1129–1135

Hu CD, Chinenov Y, Kerppola TK (2002) Visualization of interactions among bZIP and Rel family proteins in living cells using bimolecular fluorescence complementation. *Mol Cell* **9:** 789–798

Jacobson MR, Cash VL, Weiss MC, Laird NF, Newton WE, Dean DR (1989) Biochemical and genetic analysis of the nifUSVWZM cluster from *Azotobacter vinelandii*. *Mol Gen Genet* **219:** 49–57

Johnson DC, Dean DR, Smith AD, Johnson MK (2005) Structure, function, and formation of biological iron–sulfur clusters. *Annu Rev Biochem* **74:** 247–281

Kapazoglou A, Mould RM, Gray JC (2000) Assembly of the Rieske iron–sulphur protein into the cytochrome bf complex in thylakoid membranes of isolated pea chloroplasts. *Eur J Biochem* **267:** 352–360

Kobayashi K, Ehrlich SD, Albertini A, Amati G, Andersen KK, Arnaud M, Asai K, Ashikaga S, Aymerich S, Bessieres P, Boland F, Brignell SC, Bron S, Bunai K, Chapuis J, Christiansen LC, Danchin A, Debarbouille M, Dervyn E, Deuerling E, Devine K, Devine SK, Dreesen O, Errington J, Fillinger S, Foster SJ, Fujita Y, Galizzi A, Gardan R, Eschevins C, Fukushima T, Haga K, Harwood CR, Hecker M, Hosoya D, Hullo MF, Kakeshita H, Karamata D, Kasahara Y, Kawamura F, Koga K, Koski P, Kuwana R, Imamura D, Ishimaru M, Ishikawa S, Ishio I, Le Coq D, Masson A, Mauel C, Meima R, Mellado RP, Moir A, Moriya S, Nagakawa E, Nanamiya H, Nakai S, Nygaard P, Ogura M, Ohanan T, O'Reilly M, O'Rourke M, Pragai Z, Pooley HM, Rapoport G,

Rawlins JP, Rivas LA, Rivolta C, Sadaie A, Sadaie Y, Sarvas M, Sato T, Saxild HH, Scanlan E, Schumann W, Seegers JF, Sekiguchi J, Sekowska A, Seror SJ, Simon M, Stragier P, Studer R, Takamatsu H, Tanaka T, Takeuchi M, Thomaides HB, Vagner V, van Dijl JM, Watabe K, Wipat A, Yamamoto H, Yamamoto M, Yamamoto Y, Yamane K, Yata K, Yoshida K, Yoshikawa H, Zuber U, Ogasawara N (2003) Essential *Bacillus subtilis* genes. *Proc Natl Acad Sci USA* **100:** 4678–4683

Kost B, Spielhofer P, Chua NH (1998) A GFP-mouse talin fusion protein labels plant actin filaments *in vivo* and visualizes the actin cytoskeleton in growing pollen tubes. *Plant J* **16:** 393–401

Kushnir S, Babiychuk E, Storozhenko S, Davey MW, Papenbrock J, De Rycke R, Engler G, Stephan UW, Lange H, Kispal G, Lill R, Van Montagu M (2001) A mutation of the mitochondrial ABC transporter Sta1 leads to dwarfism and chlorosis in the *Arabidopsis* mutant starik. *Plant Cell* **13:** 89–100

Leon S, Touraine B, Briat JF, Lobreaux S (2002) The AtNFS2 gene from *Arabidopsis thaliana* encodes a NifS-like plastidial cysteine desulphurase. *Biochem J* **366:** 557–564

Leon S, Touraine B, Ribot C, Briat JF, Lobreaux S (2003) Iron-sulphur cluster assembly in plants: distinct NFU proteins in mitochondria and plastids from *Arabidopsis thaliana*. *Biochem J* **371:** 823–830

Lill R, Kispal G (2000) Maturation of cellular Fe–S proteins: an essential function of mitochondria. *Trends Biochem Sci* **25:** 352–356

Lill R, Muhlenhoff U (2005) Iron–sulfur–protein biogenesis in eukaryotes. *Trends Biochem Sci* **30:** 133–141

Loiseau L, Ollagnier-de-Choudens S, Nachin L, Fontecave M, Barras F (2003) Biogenesis of Fe–S cluster by the bacterial Suf system: SufS and SufE form a new type of cysteine desulfurase. *J Biol Chem* **278:** 38352–38359

Møller SG, Kunkel T, Chua NH (2001) A plastidic ABC protein involved in intercompartmental communication of light signaling. *Genes Dev* **15:** 90–103

Muhlenhoff U, Lill R (2000) Biogenesis of iron–sulfur proteins in eukaryotes: a novel task of mitochondria that is inherited from bacteria. *Biochim Biophys Acta* **1459:** 370–382

Nachin L, Loiseau L, Expert D, Barras F (2003) SufC: an unorthodox cytoplasmic ABC/ATPase required for [Fe–S] biogenesis under oxidative stress. *EMBO J* **22:** 427–437

Ollagnier-de-Choudens S, Lascoux D, Loiseau L, Barras F, Forest E, Fontecave M (2003) Mechanistic studies of the SufS–SufE cysteine desulfurase: evidence for sulfur transfer from SufS to SufE. *FEBS Lett* **555:** 263–267

Outten FW, Djaman O, Storz G (2004) A suf operon requirement for Fe–S cluster assembly during iron starvation in *Escherichia coli*. *Mol Microbiol* **52:** 861–872

Outten FW, Wood MJ, Munoz FM, Storz G (2003) The SufE protein and the SufBCD complex enhance SufS cysteine desulfurase activity as part of a sulfur transfer pathway for Fe–S cluster assembly in *Escherichia coli*. *J Biol Chem* **278:** 45713–45719

Picciocchi A, Douce R, Alban C (2003) The plant biotin synthase reaction. Identification and characterization of essential mitochondrial accessory protein components. *J Biol Chem* **278:** 24966–24975

Pilon-Smits EA, Garifullina GF, Abdel-Ghany S, Kato S, Mihara H, Hale KL, Burkhead JL, Esaki N, Kurihara T, Pilon M (2002) Characterization of a NifS-like chloroplast protein from *Arabidopsis*. Implications for its role in sulfur and selenium metabolism. *Plant Physiol* **130:** 1309–1318

Rouault TA, Tong WH (2005) Iron–sulphur cluster biogenesis and mitochondrial iron homeostasis. *Nat Rev Mol Cell Biol* **6:** 345–351

Schwartz CJ, Djaman O, Imlay JA, Kiley PJ (2000) The cysteine desulfurase, IscS, has a major role in *in vivo* Fe–S cluster formation in *Escherichia coli*. *Proc Natl Acad Sci USA* **97:** 9009–9014

Seidler A, Jaschkowitz K, Wollenberg M (2001) Incorporation of iron–sulphur clusters in membrane-bound proteins. *Biochem Soc Trans* **29:** 418–421

Studier FW (2005) Protein production by auto-induction in high-density shaking cultures. *Prot Expres Purif* **41:** 207–234

Takahashi Y, Tokumoto U (2002) A third bacterial system for the assembly of iron–sulfur clusters with homologs in archaea and plastids. *J Biol Chem* **277:** 28380–28383

Tokumoto U, Takahashi Y (2001) Genetic analysis of the *isc* operon in *Escherichia coli* involved in the biogenesis of cellular iron–sulfur proteins. *J Biochem (Tokyo)* **130:** 63–71

Xu XM, Adams S, Chua NH, Møller SG (2005) AtNAP1 represents an atypical SufB protein in *Arabidopsis plastids*. *J Biol Chem* **280:** 6648–6654

Xu XM, Møller SG (2004) AtNAP7 is a plastidic SufC-like ATP-binding cassette/ATPase essential for *Arabidopsis* embryogenesis. *Proc Natl Acad Sci USA* **101:** 9143–9148

Ye H, Garifullina GF, Abdel-Ghany S, Zhang L, Pilon-Smits EAH, Pilon M (2005) AtCpNifS is required for iron–sulfur cluster formation in ferredoxin *in vitro*. *Planta* **220:** 602–608

Zheng L, Cash VL, Flint DH, Dean DR (1998) Assembly of iron–sulfur clusters. Identification of an iscSUA–hscBA–fdx gene cluster from *Azotobacter vinelandii*. *J Biol Chem* **273:** 13264–13272